Origin of subgap states in amorphous In-Ga-Zn-O

Wolfgang Körner,[1,*] Daniel F. Urban,[1] and Christian Elsässer[1,2]

[1] *Fraunhofer Institute for Mechanics of Materials IWM, Wöhlerstr. 11, 79108 Freiburg, Germany*
[2] *Institute for Applied Materials, Karlsruhe Institute of Technology, Kaiserstr. 12, 76131 Karlsruhe, Germany*

(Dated: July 12, 2013)

We present a density–functional theory analysis of stoichiometric and nonstoichiometric crystalline and amorphous In-Ga-Zn-O (c-IGZO, a-IGZO) which connects the recently experimentally discovered electronic subgap states to structural features of a-IGZO. In particular we show that undercoordinated oxygen atoms create electronic defect levels in the lower half of the band gap up to about 1.5 eV above the valence band edge. As a second class of fundamental defects that appear in a-IGZO we identify mainly pairs of metal atoms which are not separated by oxygen atoms in between. These defects cause electronic defect levels in the upper part of the band gap. Furthermore we show that hydrogen doping can suppress the deep levels due to undercoordinated oxygen atoms while those of metal defects just undergo a shift within the band gap. Altogether our results provide an explanation for the experimentally observed effect that hydrogen doping increases the transparency and improves the conductivity of a-IGZO.

PACS numbers: 64.70.kp,68.35.bj,72.80.Ng

I. INTRODUCTION

Amorphous oxide semiconductors are promising transparent and conducting materials because their fabrication is easy and cheap. They fulfill the additional requirements for new products such as organic light emitting diodes or rollable thin-film-transistor liquid-crystal displays on flexible substrates, namely uniform morphology and low deposition temperature (below 200°C). The multi-component amorphous oxide semiconductor In-Ga-Zn-O (IGZO) has recently attracted much attention since it shows the best performance so far[1,2] concerning both electrical conductivity and optical transparency. Both properties are strongly influenced by defect structures and related energy levels, in particular if the latter lie within the band gap (subgap states).

In spite of the successful implementation of IGZO into working devices mentioned above, the origin of the subgap states in IGZO and also in related oxides remains an open question.[3–8] These subgap states may be the reason why p-type inversion operations in oxide thin-film-transistors could not be realized so far.[4] In this paper we give an answer to the question of the structural origin of these deep lying levels.

Previous theoretical investigations by Kamiya *et al.*[7–9] hint at localized defects, namely oxygen vacancies as possible sources of deep states above the valence band (VB). Our previous studies on amorphous Zn-Sn-O suggest a different picture. There, subgap states above the VB could be assigned to undercoordinated oxygen atoms, and subgap states in the upper half of the band gap to metal-metal defect complexes.[10,11] A third group of defects that create levels close to the conduction band (CB) was found to be that of defect complexes of Sn atoms with neighboring oxygen atoms which strongly deviate from perfect SnO_6 octahedra.

In the present study we show that a similar relation between the above mentioned defect-types and the resulting level structure within the band gap can be established for a-IGZO. In addition to the identification of the key defects in a-IGZO we will discuss recipes to reduce those defects. Our results can explain the experimentally seen decrease of subgap states by moving to oxygen-rich conditions or by hydrogen doping (wet annealing[6]).

The important difference with respect to previous studies on IGZO[7–9] is our use of a self-interaction corrected (SIC) local-density approximation (LDA) to density functional theory (DFT). This choice is motivated by recent theoretical work[12–15] which has shown that both,

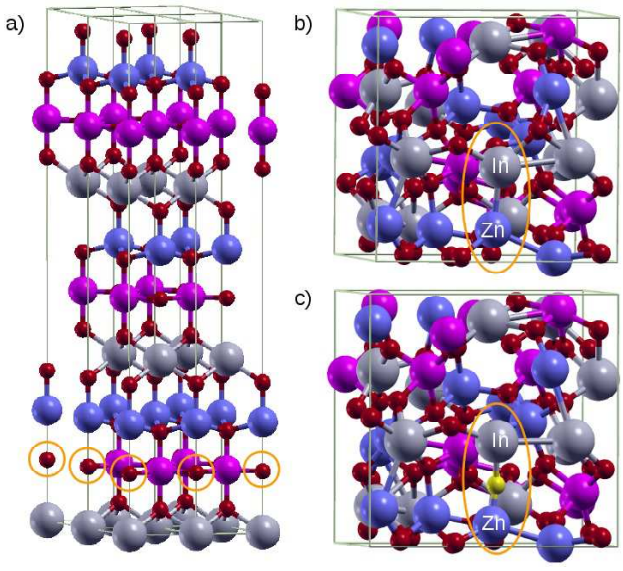

FIG. 1: (Color online) Crystal structure of (a) four supercells of c-IGZO, (b) one supercell of a-IGZO:V_O (sample B) including an oxygen vacancy V_O and (c) a-IGZO:$V_{O(anh)}$ (sample B) additionally doped with a hydrogen atom. Large grey, purple and blue spheres represent In, Ga and Zn atoms, respectively. Small red spheres represent oxygen atoms, and the small yellow sphere in c) represents a hydrogen atom.

LDA and the generalized gradient approximation (GGA), have limited predictive power for wide band gap semiconductors due to their inherent artificial self-interaction. SIC–LDA overcomes this limitation and yields electronic band strucures and corresponding band gaps that are in good agreement with experiments.[12] Moreover, SIC–LDA is numerically efficient and only requires little more resources that standard LDA calculations. In this aspect it outruns the various available hybrid functionals which have in common to become computationally very demanding for the large supercells needed to thoroughly model amorphous structures.

The paper is organized as follows. Section II is dedicated to the theoretical framework of the SIC–LDA and the numerical generation of amorphous structures. Our results on atomic and electronic structures are presented and discussed in Sec. III. Finally, Sec. IV gives a summary and conclusions.

II. THEORETICAL APPROACH

A. SIC-LDA calculations

The total-energy and electronic-structure calculations in this work are performed on the basis of DFT using the computational mixed-basis pseudopotential (MBPP) method[17–20] with the same calculation setup as in our previous papers.[10,12,13] We have taken the LDA for exchange-correlation as parameterized by Perdew and Zunger.[21] For the ionic cores of In, Ga, Zn, and O optimally smooth norm–conserving pseudopotentials[22] and for the electronic bands a mixed basis of plane waves and nonoverlapping localized orbitals were used. Due to the localized orbitals a plane–wave cutoff energy of 20 Ry (1Ry = 13.606 eV) is sufficient to obtain converged results. For the k-point sampling of the Brillouin-zone integrals a Monkhorst-Pack mesh of $3 \times 3 \times 3$ points and a Gaussian broadening of 0.2 eV were used. The electronic DOS of the supercells were evaluated with the same mesh and a Gaussian smearing of 0.1 eV. In order to compare the DOS for different samples, we aligned the curves according to the low lying Zn 3d band and set the VB edge of c-IGZO to 0 eV.

We corrected the self-interaction problem of LDA by an incorporation of the SIC into the pseudopotentials. This approach is explained in detail in Refs. 12 and 23. The SIC procedure depends on the weight factors w_l accounting for occupation of the individual s, p and d valence orbitals. For c-$InGaZnO_4$ and a-$InGaZnO_4$, correcting only occupied In 4d, Ga 3d, Zn 3d, O 2s and 2p states, we used In(0, 0, 1), Ga(0, 0, 1), Zn(0, 0, 1) and O(1, 0.85, 0) where the bracket terms denote (w_0, w_1, w_2). Furthermore, we have reduced the atomic SIC by a factor $\alpha = 0.8$ for all the oxides considered in this paper. The electronic structures obtained with this choice of parameters are discussed and compared to experiments in Sec. III B and Sec. III C.

ion pair	A_{ij}(eV)	ρ_{ij}(Å)	C_{ij}(eV·Å^6)
In^{+3} – O^{-2}	1293.600	0.331	4.325
Ga^{+3} – O^{-2}	2339.766	0.274	0.0
Zn^{+2} – O^{-2}	600.300	0.337	0.0
O^{-2} – O^{-2}	25.41	0.694	32.32

TABLE I: Parameters of the Buckingham potential $V_{ij} = A_{ij} \cdot \exp(-r_{ij}/\rho_{ij}) - C_{ij} r_{ij}^{-6}$ used for the molecular dynamics simulations, taken from Ref. 16.

B. Model for crystalline and amorphous In-Ga-Zn-O

As reference and starting point for the generation of the amorphous model systems we constructed a 84 atoms supercell of crystalline $InGaZnO_4$ (space group R-3m).

Following methodologically the pioneering work of Nomura et al.,[24] we generated eight stoichiometric amorphous $InGaZnO_4$ structures by means of classical molecular dynamics (MD) simulations with the GULP code.[25] Empirical rigid-ion potentials of Buckingham type were employed. The corresponding potential parameters are given in Table I. The MD simulations were started at 5000 K and subsequently cooled down in steps of 10 K per ps with time steps of 2 fs at constant temperature and constant volume. The obtained structures were relaxed subsequently by LDA.

In order to study oxygen-poor amorphous structures we removed one O atom from the individual equlibrated stoichiometric amorphous supercells and also relaxed by LDA. The resulting ensemble of eight samples are denoted by a-IGZO:V_O(samples A − H). This first set can be seen as a grown stoichiometric film which is treated subsequently in oxygen-poor atmosphere. A second set of oxygen deficient amorphous samples was obtained by initially removing an O atom performing the same MD heating and cooling procedure followed by LDA relaxation. This second set simulates film growth under oxygen-poor conditions and is denoted by a-IGZO:$V_{O(anh)}$(samples A − H) referring to the oxygen hole being annihilated by the MD.

Further details on this procedure are given in the Refs. 10 and 11.

III. RESULTS AND DISCUSSION

A. Atomic structure

The calculated structural parameters of the single crystal a=3.32 Å and c = 25.54 Å deviate by less than 2 percent from experimental values a = 3.2948 Å and c = 26.071 Å.[26] Due to the smaller volume of our LDA optimized c-IGZO structure our mass density of 6.43 g/cm^3

is slightly larger than the experimental value of 6.379 g/cm^3.[26] On average our amorphous samples have a volume increase of 11.3 % relative to c-IGZO leading to an average mass density of 5.77 g/cm^3 which is close to the value 5.9 g/cm^3 observed in experiments.[24]

Table II contains the coordination numbers of the c- and a-IGZO samples. Concerning c-IGZO the Zn atoms are in tetrahedral positions with Zn-O distances of 1.96 to 1.99 $\AA$. A fifth O atom marked by an orange circle in Fig. 1 is at 2.48 $\AA$ in c-direction. The difference in coordination numbers of c-IGZO with respect to Ref. 28 for Ga and Zn comes from the different definition of the cut-off values. We have chosen a value of 3$\AA$ for the metal oxygen pairs.

The average coordination numbers of our amorphous samples given in Table II appear reasonable because In and Ga ions usually occupy octahedral positions whereas Zn ions take tetrahedral sites. This tendency is reflected in coordination numbers of about 5 for In and Ga and a coordination number closer to 4 for Zn. Interestingly, the experimental value for the coordination number of Zn-O determined from extended x-ray absorption fine structures (EXAFS) exceeds the coordination numbers for In-O and Ga-O. Nevertheless, Nomura et al.[24] conclude that the Zn ions preferentially have fourfold coordination while In and Ga have fivefold and sixfold coordination. Our a-IGZO samples are fully in line with this coordination statement although our and their coordination numbers do not coincide. Finally, oxygen has mostly tetrahedral coordination. In summary, our amorphous structure samples appear to be reasonable with respect to available experimental information. They are thus a good fundament for the analysis of the electronic structure of a-IGZO.

coordination numbers	c-$InGaZnO_4$	a-$InGaZnO_4$
In–O	6 (6^a)	5.24 ($\sim$ 5^b, $\sim$ 4.5^c)
Ga–O	5 (4^a)	4.90 ($\sim$5^b, $\sim$4.3^c)
Zn–O	5 (4^a)	4.41 ($\sim$4^b, $\sim$4.6^c)
O–O	12	10.38
O–(In, Ga, Zn)	4 (4^a)	3.64

TABLE II: Coordination numbers of the LDA-relaxed crystalline and amorphous IGZO structures. The given values for the amorphous compounds are the averages of the eight stoichiometric samples generated. Our cut-off value was 3.7$\AA$ for O-O pairs and 3$\AA$ for In-O, Ga-O and Zn-O pairs. The values in brackets for c-IGZO marked by ^{a} are from Ref. 28 and differ from ours due to different choice of cut-off radii. For a-IGZO the values marked by ^{b} and ^{c} are the LDA-relaxed and experimentally determined EXAFS values of Ref. 24.

Structure	E_g^{exp}			E_g^{SIC}	E_g^{LDA}	E_g^{HSE06}
c-$InGaZnO_4$	3.05^a	3.5^b	3.68^c 3.7^d	3.50	1.36	3.06^f
a-$InGaZnO_4$		3.10^c	3.1^e	2.72	0.98	2.24^f

TABLE III: Comparison of the experimentally and theoretically determined electronic band gaps E_g (^{a} Ref. 29, ^{b} Ref. 16, ^{c} Ref. 30. ^{d} Ref. 8, ^{e} Ref. 31 ^{f} Ref. 32). All energies are given in eV. The LDA and SIC band gap values of the amorphous structures are the averages of the 8 stoichiometric samples.

B. Band gaps of c-IGZO and a-IGZO

Experimental and theoretical values for the band gaps of c-IGZO and a-IGZO are listed in Table III. The experimentally determined band gap of 3.68 eV for c-IGZO of Ref. 30 has probably the highest accuracy since that very recent study was focused especially on the determination of the band structure. All the other available theoretical band gap values lie below this value. However, the SIC approach underestimates the band gap only by a few percent and thus describes the electronic structure of c-IGZO rather well.

For a-IGZO Ref. 30 reports a band gap of 3.10 eV which means a reduction of about 20% compared to c-IGZO. The band gap values obtained from DFT with either the HSE06-functional or the SIC approach, both can be considered as approximately in line with that amount of reduction with respect to c-IGZO. This reduction of the band gap is mainly caused by a VB tail which is illustrated in Fig. 2 comparing the total DOS of c-IGZO to the one of Sample A of our a-IGZO set. Sample A has a VB tail of about 1 eV and a negligible CB tail which indicates that the reduction of the band gap is dominated by modifications of VB states.

The spherical s orbitals forming mainly the CB are rather insensitive to structural disorder and thus lead to small CB tails. On the other hand, the upper part of the VB is formed mainly of direction-dependent O 2p orbitals which are influenced more strongly by disorder which therefore results in significantly bigger tails.[1,32]

C. Subgap states in a-IGZO

The DOS of our stoichiometric and oxygen poor a-IGZO samples all show the characteristic tails attributed to the general disorder as discussed in the previous section. However, several localized deep levels of different origin appear above those tails We observe an increasing probablity to find such deep levels when going from stoichiometric to oxygen poor a-IGZO samples. Only 2 of the 8 stoichiometric samples show deep levels compared to 15 of the 16 oxygen poor samples.

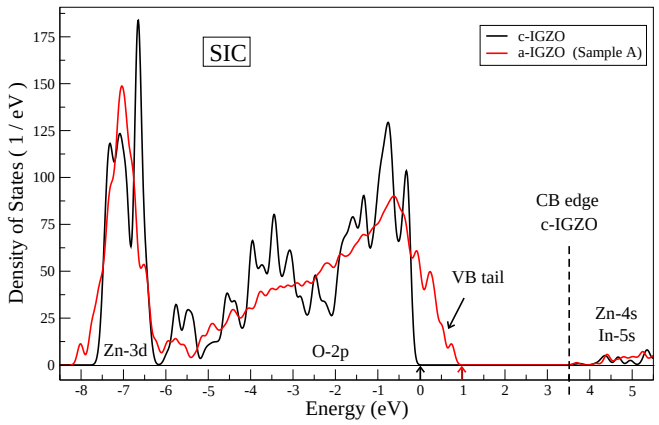

FIG. 2: (Color online) Comparison of the total DOS of c-IGZO and a-IGZO (sample A) determined with SIC-LDA. The small colored arrows below the zero line indicate the occupation level (Fermi level) for each supercell. Sample A is a typical representative of our set of stoichiometric a-IGZO. It has deep levels above the VB which form a VB tail with a width of about 1 eV. Moreover the CB edge of sample A almost coincides with c-IGZO reflecting the little influence of the disorder on the CB s-states.

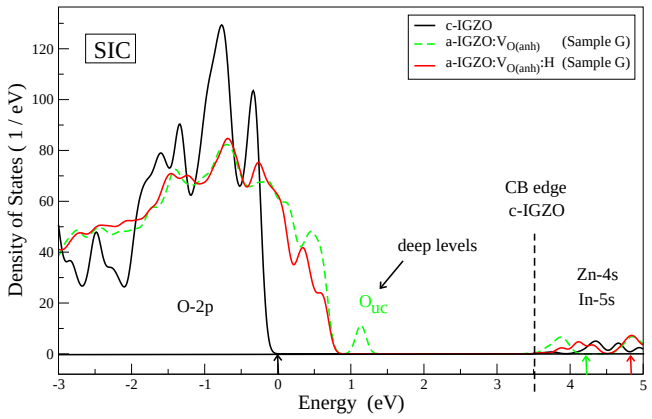

FIG. 3: (Color online) Total DOS of oxygen poor a-IGZO:$V_{O(anh)}$ (sample G) with and without hydrogen, as calculated with SIC-LDA. The DOS of c-IGZO is shown as reference. The small colored arrows below the zero line indicate the occupation level (Fermi level) for each supercell. The deep level originating from the undercoordinated O atom (O_{uc}) is clearly separated from the VB tail (c.f. green dashed line). Doping with hydrogen makes these deep levels disappear (solid red line)

1. *Undercoordinated O atoms*

A defect complex which is frequently encountered in our oxygen poor samples is that of an undercoordinated O atom. A representative example of the corresponding DOS is shown in Fig. 3 for the case of a-IGZO:V_O (sample G). The origin of the subgap state can be directly linked to an specific undercoordinated O atom by means of an analysis of the local DOS of all the individual atoms.

In contrast, in the LDA analysis of IGZO by Kamiya et al.[7,8] the deep fully-occupied localized states above the VB are linked to oxygen vacancies, instead. As already discussed in our previous paper[11] on Zn-Sn-O we agree with Kamiya et al. concerning the LDA results. However, as already mentioned, standard LDA is known not to be reliable for these oxide systems.[12–15] Taking into account the SIC which presumably leads to a more accurate and reliable picture we can assign in our a-IGZO samples all the deep levels in the lower half of the band gap up to about 1.5 eV to undercoordinated oxygen atoms.

2. *Misscoordinated metal atoms*

A second class of defect states is related to oxygen vacancies/deficiencies situated nearby one, two or three metal atoms. Sketches of generic defects of one or two metal atoms are given in Fig. 4. According to our SIC analysis, the corresponding deep levels lie in the upper half of the band gap. The DOS of several oxygen poor a-IGZO samples that show defect states of that kind is presented in Fig. 5. Note that these DOS results fit excellently to the theoretical considerations of Robertson

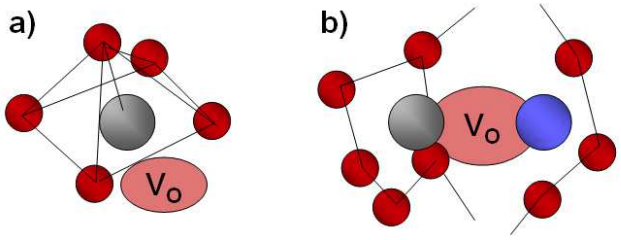

FIG. 4: (Color online) a) Sketch of a typical one metal defect. A 1In defect consist of a In atom (grey) surrounded by 4 or 5 O atoms (red). The void near the In atom can be interpreted as oxygen vacancy (V_O). b) Sketch of a metal-metal defect that is characterized by for example by a In and a Zn atom (blue) which lie next to each other without any separating O atom in between.

summarized in the sketch of Fig. 5 of Ref. 32.

The most frequently encountered two metal defect in our a-IGZO samples with annihilation steps is the In-Zn defect (seven out of eight). One example of a structure with this defect is shown in Fig.1b. Between the In and Zn atoms of interest there is no separating O atom and their distances are between 2.58–3.60 $\AA$. The lacking O atom can be interpreted as oxygen vacancy. The deep levels produced by the In-Zn defect of sample a-IGZO:$V_{O(anh)}$ are shown in Fig. 6. The energy positions of these defects are not unique. They varied for the seven different In-Zn defect levels in between 3.2 and 3.7 eV above the VB.

Another example are Sample B (green dashed line in Fig. 5) and sample C (blue solid line in Fig. 5) which both contain a Ga-Zn defect. The energy positions of these defect levels differ by more than 0.5 eV. It is clear that the

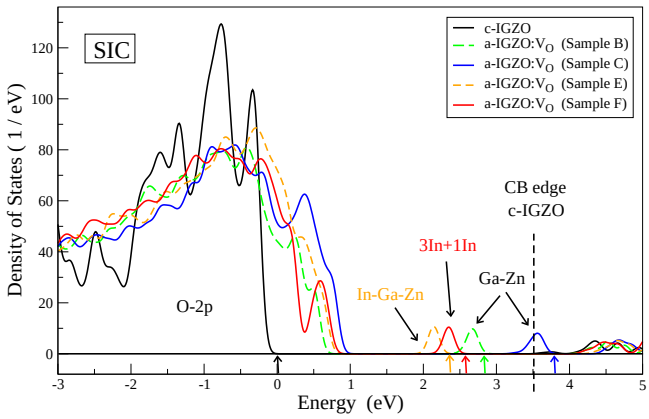

FIG. 5: (Color online) Total DOS of various oxygen poor a-IGZO samples as calculated with SIC-LDA. The DOS of c-IGZO is shown as reference. Small colored arrows below the zero line indicate the occupation levels. The different multiple metal defects lead to defect levels in the upper half of the band gap.

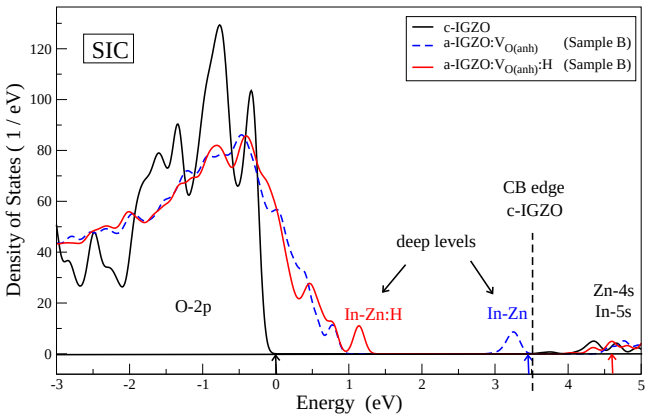

FIG. 6: (Color online) Total DOS of oxygen poor a-IGZO:V$_{O(anh)}$ (sample B) with and without hydrogen, as calculated with SIC-LDA. The DOS of c-IGZO is shown as reference. Small colored arrows below the zero line indicate the occupation levels. The In-Zn pair defect creates a defect levels below the CB edge (blue dashed line). Doping with hydrogen moves these deep levels into the VB (solid red line) and additionally moves up the Fermi energy.

energy position of a defect level is not only determined by species and number of metal atoms directly involved but also by the whole local arrangement around the oxygen hole.

Interestingly, we have found only a single one metal-atom defect in our a-IGZO samples, namely a 1In-defect, i.e. a miscoordinated In atom (see red line in Fig. 5). This is different from our study of a-Zn-Sn-O[10,11] in which we have found that the 1Sn defect (structure shown Fig. 4a) is the most frequent defect in a-Zn-Sn-O.

The 1In defect appears in a-IGZO:V$_O$ (sample F) in addition to a 3In defect in which 3 In atoms surround an oxygen hole. A second even deeper lying three-metal-atom defect is the In-Ga-Zn defect in a-IGZO:V$_O$ (sample E) shown in Fig. 5 (dashed orange line). It is the deepest lying defect related to an oxygen vacancy that was found in our set of amorphous samples.

Looking at the defect formation energies following methodically Refs. 8 and 9 we obtain an average defect formation energy of 3.4 eV for the In-Zn defect. All the other defects have higher formation energies between 3.8 and 5 eV which fits well to the range 3.3 to 4.7 eV found by Kamiya et al.[9] for defects related to oxygen vacancies. Thus we expect the In-Zn defect to be the dominant defect in this group of defects responsible for the subgap states in the upper half of the band gap.

In summary, our analysis of the subgap states even quantitatively agrees with the experimental findings. We relate the experimental subgap DOS[3] which continuously extends from the VB to about 1.5 eV to undercoordinated O atoms while the extra subgap DOS 0.1-0.3 eV below the CB minimum observed in Ref. 5 corresponds well to the In-Zn defect levels (see Fig. 6).

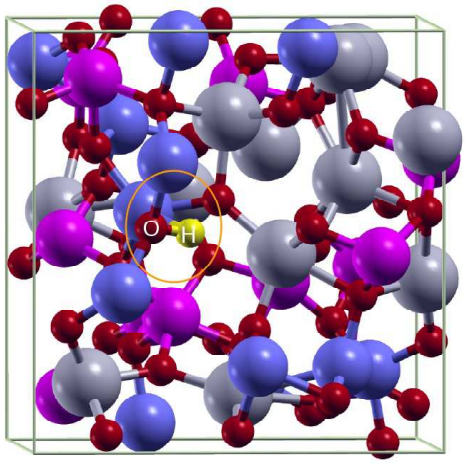

FIG. 7: (Color online) Supercell of a-IGZO:V$_{O(anh)}$ (sample G) additionally doped with hydrogen. Large grey, purple and blue spheres represent In, Ga and Zn atoms, respectively. Small red spheres represent oxygen atoms and the small yellow sphere represents a hydrogen atom. The orange circle highlights the O-H bond that is formed.

3. *Impact of hydrogen doping on the subgap states*

As mentioned in the previous section we observe an increase in the number of deep defect levels found when going from stoichiometric to oxygen poor samples. Since the presence of these deep levels in general reduces the transparency of the material[6] it is desirable to have a procedure at hand which reduces the number of deep levels inside the band gap. One possibility is the annealing in an oxygen-rich atmosphere which was proven to indeed have a positive effect, see e.g. Ref. 6. However, the reduction of subgap states and thus an increase in transparency

is usually paid by a decrease in conductivity since oxygen deficiencies forming donor states are suppressed.[33]

Another possibility is the treatment with additional hydrogen (like by experimental wet annealing[6]). In order to simulate this we have added H atoms to the supercells containing the discussed point defects and have subsequently relaxed the structures. A hydrogen atom near the undercoordinated oxygen atom results in the disappearance of the localized deep levels into the VB (compare the green dashed and red solid lines in Fig. 3). This is achieved via saturating the oxygen through the creation of an O-H bond with a relaxed length of about 1.0 $\AA$ (see Fig. 7). Such a disappearance of deep levels above the VB is also observed in experiments (see Fig. 3b of Ref. 6) which corroborates our theory of undercoordinated oxygen atoms.

On the other hand, hydrogen doping is not efficient for the defects related to oxygen vacancies. For all our model structures we have observed the behavior exemplified for a-IGZO:V_O (sample B) in Fig. 6. The deep levels due to the In-Zn defect move down in energy but remain deep and well visible above the VB tail. The atomic structure of the In-Zn-H defect is shown in Fig. 1c. The hydrogen atom relaxes to a position between the metal atoms and increases their distance.

A further, general effect of H doping is the upshift of the Fermi level (see arrows in Fig. 3 and Fig. 6). The supply of extra charge carriers and a Fermi level near the conduction band should increase the electrical conductivity of a-IGZO. Indeed this behavior was already observed experimentally.[34,35]

IV. SUMMARY AND CONCLUSIONS

We have studied the atomic structures, formation energies and electronic densities of states of stoichiometric and nonstoichiometric c- and a-IGZO model structures using a SIC-LDA approach.

According to our calculations the subgap states can be divided into two main groups. In the lower half of the band gap the deep localized defect levels are related to undercoordinated O atoms. The subgap states in the upper part of the band gap are caused by defects related to oxygen vacancies. The latter defect levels originate mostly from pairs of metal atoms which come close without a separating oxygen atom in between.

Our simulation of the addition of hydrogen reveals that deep defect levels due to undercoordinated O atoms can be efficiently suppressed which is in accordance with experiments.[6] Hydrogen atoms preferably bind to the undercoordinated O atoms and compensate the electron deficit. The addition of hydrogen to the defects related to oxygen vacancies on the other hand shifts the electronic defects from the upper half to the lower half of the band gap but these levels do not dissappear into the VB. Nevertheless, altogether hydrogen doping increases the transparency of a-IGZO. Furthermore, we have shown that hydrogen doping shifts the Fermi level to the conduction band which improves the conductivity of a-IGZO.[34,35]

Acknowledgments

Financial support for this work was provided by the European Commission through contract No. NMP3-LA-2010-246334 (ORAMA).

* Electronic address: wolfgang.koerner@iwm.fraunhofer.de

[1] K. Nomura, H. Ohta, A. Takagi, T. Kamiya, M. Hirano and H. Hosono, Nature (London), **432**, 488 (2004).

[2] H. Yabuta, M. Sano, K. Abe, T. Aiba, T. Den, H. Kumomi, K. Nomura, T. Kamiya and H. Hosono, Appl. Phys. Lett. **89**, 112123 (2006).

[3] H.-H Hsieh, T. Kamiya, K. Nomura, H. Hosono and C.-C. Wu, Appl. Phys. Lett. **92**, 133503 (2008).

[4] K. Nomura, T. Kamiya, H. Yanagi, E. Ikenaga, K. Yang, K. Kobayashi, M. Hirano and H. Hosono, Appl. Phys. Lett. **92**, 202117 (2008).

[5] M. Kimura, T. Nakanishi, T. Kamiya, K. Nomura and H. Hosono, Appl. Phys. Lett. **92**, 133512 (2008).

[6] K. Nomura, T. Kamiya, E. Ikenaga, H. Yanagi, K. Kobayashi and H. Hosono, J. Appl. Phys. **109**, 073726 (2011).

[7] T. Kamiya, K. Nomura, M. Hirano and H. Hosono, Phys. Stat. Sol. C **5**, 3098 (2008).

[8] T. Kamiya, K. Nomura and H. Hosono, Phys. Stat. Sol. A **206**, 860 (2009).

[9] T. Kamiya, K. Nomura and H. Hosono, Phys. Stat. Sol. A **207**, 1698 (2010)

[10] W. Körner, P. Gumbsch and C. Elsässer, Phys. Rev. B **86**, 165210 (2012).

[11] W. Körner and C. Elsässer, Thin Sol. Films, http://dx.doi.org/10.1016/j.tsf.2013.05.146 (2013).

[12] W. Körner and C. Elsässer, Phys. Rev. B **81**, 085324 (2010).

[13] W. Körner and C. Elsässer, Phys. Rev. B **83**, 205306 (2011).

[14] P. Rinke, A. Janotti, M. Scheffler and C. G. Van de Walle, Phys. Rev. Lett. **102** , 026402 (2009).

[15] S. J. Clark, J. Robertson, S. Lany and A. Zunger, Phys. Rev. B **81**, 115311 (2010)

[16] M. Orita, H. Tanji, M. Mizuno, H. Adachi, and I. Tanaka, Phys. Rev. B **61**, 1811 (2000).

[17] C. Elsässer, N. Takeuchi, K. M. Ho, C. T. Chan P. Braun

and M. Fähnle, J. Phys.: Condens. Matter **2**, 4371 (1990).
[18] K. M. Ho, C. Elsässer, C. T. Chan and M. Fähnle, J. Phys.: Condens. Matter **4**, 5189 (1992).
[19] B. Meyer, K: Hummler, C. Elsässer and M. Fähnle, J. Phys. Condens. Matter **7**, 9201-9217 (1995)
[20] F. Lechermann, M. Fähnle, B. Meyer and C. Elsässer Phys. Rev. B **69**, 165116 (2004).
[21] P. Perdew and A. Zunger, Phys. Rev. B **23**, 5048 (1981).
[22] D. Vanderbilt, Phys. Rev. B **32**, 8412 (1985).
[23] D. Vogel, P. Krüger and J. Pollmann, Phys. Rev. B **54**, 5495 (1996).
[24] K. Nomura, T. Kamiya, H. Ohta, T. Uruga, M. Hirano and H. Hosono, Phys. Rev. B **75**, 035212 (2007).
[25] J. D. Gale, J. Chem. Soc., Faraday Trans. **93**, 629 (1997).
[26] N. Kimizuka and T. Mohri, J. Sol. St. Chem. **60**, 382 (1985)
[26] K. Kato, I. Kawada, N. Kimizuka, and T. Katsura, Z. Kristallogr. **141**, 314 (1975).
[28] J. E. Medvedeva and C. L. Hettiarachchi, Phys. Rev. B **81**, 125116 (2010).
[29] C.-S. Chuang, T. C. Fung, B. G. Mullins, K. Nomura, T. Kamiya, H.-P. D. Shieh, H. Hosono, and J. Kanicki: SID Int. Symp. Dig. Tech. Pap. **39**, 1215 (2008).
[30] K. Lee, K. Nomura, H. Yanagi, T. Kamiya, E. Ikenaga, T. Sugiyama, K. Kobayashi and H. Hosono, J. Appl. Phys. **112**, 033713 (2012)
[31] J. Yao, S. Zhang and L. Gong, Appl. Phys. Lett. **101**, 093508 (2012)
[32] A. Walsh, J. L. F. Da Silva and S.-H. Wei, Chem. Mat. **21**, 5119 (2009).
[32] J. Robertson, Phys. Stat. Solidi. B **245**, 1026 (2009).
[33] M. K. Jayaraj, K. J. Saji, K. Nomura, T. Kamiya and H. Hosono, J. Vac. Sci. Technol. B **26**, 495 (2008).
[34] B. D. Ahn, H. S. Shin, H. J. Kim, J.-S. Park and J. K. Jeong, Appl. Phys. Lett. **93**, 203506 (2008).
[35] A. Sato, K. Abe, R. Hayashi, H. Kumomi, K. Nomura, T. Kamiya, M. Hirano, and H. Hosono Appl. Phys. Lett. **94**, 133502 (2009).